

Received:  
14 May 2020Revised:  
06 August 2020Accepted:  
07 August 2020<https://doi.org/10.1259/bjr.20200562>

Cite this article as:

Tunariu N, Blackledge M, Messiou C, Petralia G, Padhani A, Curcean S, et al. What's New for Clinical Whole-body MRI (WB-MRI) in the 21st Century. *Br J Radiol* 2020; **93**: 20200562.

## BJR 125<sup>TH</sup> ANNIVERSARY: REVIEW ARTICLE

# What's New for Clinical Whole-body MRI (WB-MRI) in the 21st Century

<sup>1,2</sup>NINA TUNARIU, FRCR, MD, <sup>3</sup>MATTHEW BLACKLEDGE, PhD, <sup>1</sup>CHRISTINA MESSIOU, FRCR, MD, <sup>4</sup>GIUSEPPE PETRALIA, <sup>5</sup>ANWAR PADHANI, FRCR, FRCP, <sup>1</sup>SEBASTIAN CURCEAN, MD, <sup>1,2</sup>ANDRA CURCEAN, MD and <sup>2</sup>DOW-MU KOH, FRCR, MD

<sup>1</sup>Department of Radiology, Royal Marsden Hospital, Downs Road, Sutton, London, UK

<sup>2</sup>Drug Development Unit, The Institute of Cancer Research, 15 Cotswold Road, Sutton, London, UK

<sup>3</sup>Department of Radiotherapy, The Institute of Cancer Research, 15 Cotswold Road, Sutton, London, UK

<sup>4</sup>Department of Radiology, European Institute of Oncology, Via Ripamonti, 435 - 20141 Milan, Italy

<sup>5</sup>Mount Vernon Hospital, The Paul Strickland Scanner Centre, Rickmansworth Road, Northwood, Middlesex, UK

Address correspondence to: Dr Dow-Mu Koh

E-mail: [dowmukoh@icr.ac.uk](mailto:dowmukoh@icr.ac.uk)

### ABSTRACT

Whole-body MRI (WB-MRI) has evolved since its first introduction in the 1970s as an imaging technique to detect and survey disease across multiple sites and organ systems in the body. The development of diffusion-weighted MRI (DWI) has added a new dimension to the implementation of WB-MRI on modern scanners, offering excellent lesion-to-background contrast, while achieving acceptable spatial resolution to detect focal lesions 5 to 10 mm in size. MRI hardware and software advances have reduced acquisition times, with studies taking 40–50 min to complete.

The rising awareness of medical radiation exposure coupled with the advantages of MRI has resulted in increased utilization of WB-MRI in oncology, paediatrics, rheumatological and musculoskeletal conditions and more recently in population screening. There is recognition that WB-MRI can be used to track disease evolution and monitor response heterogeneity in patients with cancer. There are also opportunities to combine WB-MRI with molecular imaging on PET-MRI systems to harness the strengths of hybrid imaging. The advent of artificial intelligence and machine learning will shorten image acquisition times and image analyses, making the technique more competitive against other imaging technologies.

### INTRODUCTION

Whole-body MRI (WB-MRI) offers wide anatomical coverage and high contrast-resolution imaging for multi-system disease evaluation. Increasing awareness of the hazards associated with ionising radiation<sup>1,2</sup> coupled with technological advances in MRI such as parallel imaging for faster image acquisition and improved image signal-to-noise ratio (SNR), have contributed to WB-MRI as a clinical tool.

Emerging indications for WB-MRI include: (a) cancer screening in population with genetic predisposition;<sup>3</sup> (b) cancer staging as a “one-stop-shop” in selected cancer types;<sup>4,5</sup> (c) imaging in children,<sup>6</sup> pregnant females<sup>7</sup> and specific genetic disorders to avoid ionising radiation; (d) for identifying malignant bone marrow disease and response assessment; and detecting complications such as fractures or spinal cord compression;<sup>8–11</sup> and (e) non-oncological inflammatory conditions such as spondyloarthropathies<sup>12</sup> and myopathies.<sup>13</sup>

In this review, we discuss the technical considerations for performing WB-MRI. We survey the application of WB-MRI for disease screening, both in the general population and in higher risk populations. The expanding role of WB-MRI in oncological diseases and the potential for WB-MRI to inform non-oncological diseases are reviewed.

### TECHNICAL CONSIDERATIONS AND IMAGING PROTOCOL

WB-MRI protocols utilize combinations of T1W, short-tau inversion recovery (STIR) T2W and diffusion-weighted (DW) sequences. T1W imaging may be performed with or without contrast enhancement.<sup>4–6,12–15</sup> Variabilities in the imaging protocols reflect different clinical indications, as well as the challenges of implementing WB-MRI across platforms, being more challenging on older systems and at 3T.

DWI is emerging as a core sequence in WB-MRI protocols as good image quality can be achieved on most modern MR

systems. The sequence is sensitive to tissue cellularity and cell viability, which shows increased signal intensity relative to background on high b-value images. Furthermore, DWI allows the quantification of the apparent diffusion coefficient (ADC; unit:  $\mu\text{m}^2/\text{s}$ ) value that aids disease characterisation and treatment response assessment. DWI shows higher accuracy for detecting bone metastases<sup>16</sup> and muscle oedema<sup>17</sup> compared with STIR. An optimized DWI protocol has high sensitivity for detecting lesions and can reduce the need for contrast medium administration. This is particularly important since there is an FDA drug safety warning for gadolinium retention using gadolinium-based contrast agents, including in the brain, for months to years after contrast administration.<sup>18</sup>

The anatomical coverage of WB-MRI usually spans “vertex to upper thigh”. However, the coverage can be extended from the vertex to the feet and including proximal upper limbs with longer acquisition time where appropriate, such as in high-risk population screening, when evaluating diseases that frequently involve long bones<sup>19</sup> or when suspecting soft tissue disease in melanoma patients.<sup>20</sup> Using coronal versus axial acquisition; or combination of both, depends on many factors including scanner performance and radiologist preferences. Axial imaging is often preferred, acquiring images in matching slice thickness (5–6 mm) to facilitate lesion correlation, while sagittal spinal imaging provides assessment for vertebral fractures and cord compression in bone disease. Technical developments such as ultrashort echo time MRI of the lung and 3D T1 sequences supplemented by fat fraction images for rib imaging aim to improve the detection of subcentimetre lung and rib metastases on WB-MRI. However, these areas remain challenging, and in relevant clinical situations, a complementary low-dose CT thorax is advocated.

There is no special preparation needed for a WB-MRI examination and the study can be undertaken on 1.5T and 3T scanners,<sup>21</sup>

although DWI image quality is more consistent at 1.5T. For patients with an implanted metallic endoprosthesis, 1.5T is preferred over 3T MRI due to less artefacts. The patient is usually scanned supine with arms by their side and knees bent with support to increase comfort. Sedation or general anaesthesia (GA) may be required in children although alternative techniques such as “feed-and-wrap” protocols or play therapy<sup>22</sup> have been successfully used.

Advances in coil technology and parallel imaging reduce acquisition time and increase image signal-to-noise. These allow a WB-MRI study from the skull vertex to mid-thigh (analogous coverage to a typical PET-CT examination) to be completed in 40 to 50 min (by comparison, a complex one body part MRI protocol can take 30 min). Automated “set up and go” acquisition protocols with in-line image composing facilitate image display and reading. Publications have highlighted good patient acceptance of the technique; with the willingness to trade slightly longer examination times for faster and more accurate diagnoses.<sup>23–25</sup>

The last few years have seen concerted efforts to define the core imaging sequences for WB-MRI (Table 1, [Supplementary Material 1](#)) using DWI as the key sequence for disease assessment<sup>26</sup> (Figure 1). As with any imaging technique, implementation of an optimised imaging protocol, radiologists training and a high level of reporting, such as using consensus reporting criteria are crucial. Current consensus reporting criteria include MET-RADS-P for advanced prostate cancer,<sup>9</sup> MY-RADS for multiple myeloma<sup>8</sup> and Whole-Body Score for Inflammation in Peripheral Joints and Enteses in Inflammatory Arthritis (MRI-WIPE).<sup>27</sup>

## WB-MRI FOR DISEASE SCREENING

### Healthy population

Preventive medicine plays an important role for healthier living. WB-MRI is an ionising radiation-free technique that can be

Figure 1. Example of a typical WB-MRI protocol including axial DWI (3 b values and ADC map), axial T1W and T2W, CAIPIRINHA (Controlled Aliasing in Parallel Imaging Results in Higher Acceleration)-derived relative fat fraction and sagittal T1W and T2W spine images. Note the sagittal spine images were acquired without anterior saturation bands to visualise the sternum. The inverted coronal 3D b900 MIP and FDG-PET images show similar anatomical coverage between techniques.

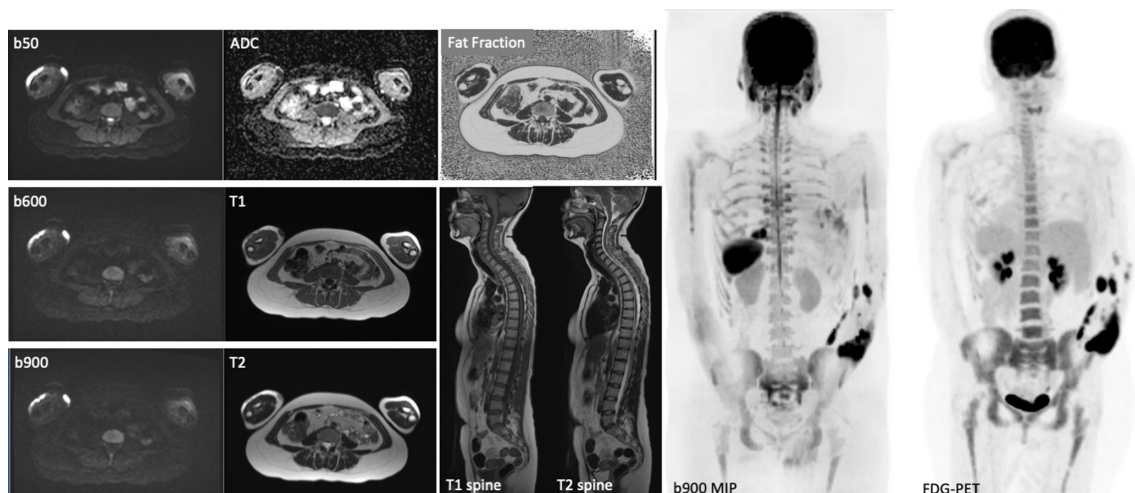
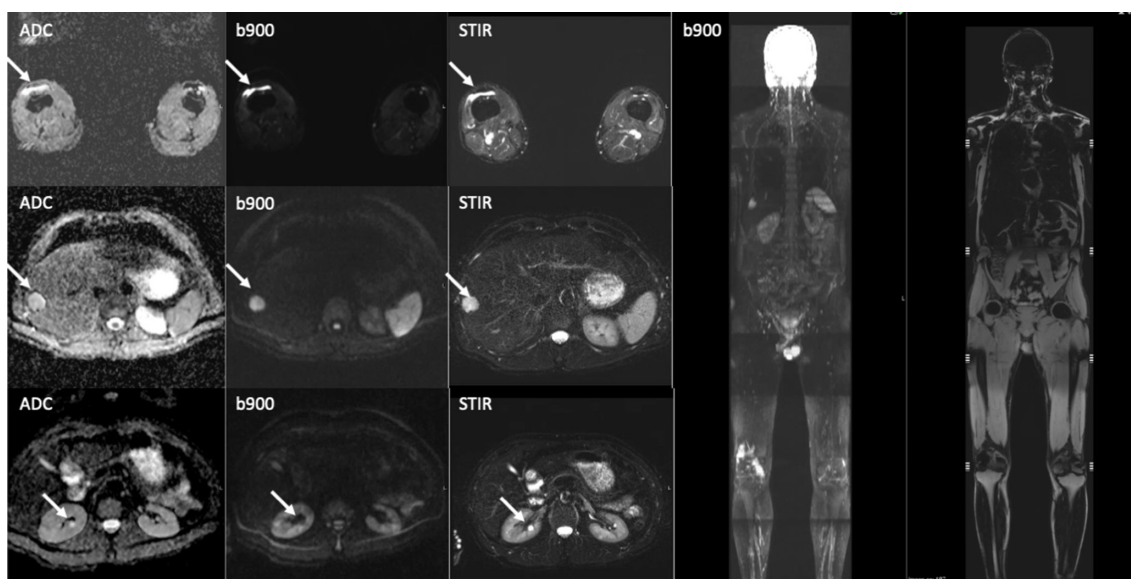


Figure 2. A screening whole body-MRI in a healthy male volunteer showing incidental benign renal cysts, hepatic haemangioma and a right knee effusion (white arrows). The liver haemangioma was confirmed on ultrasound examination.



used to screen asymptomatic individuals for malignant/non-malignant diseases, thus impacting on health outcomes.<sup>28,29</sup>

There is emerging data on the role of WB-MRI for screening the normal population. In a retrospective study of 229 patients<sup>30</sup> who underwent WB-MRI for routine health examination and cancer screening, two cases of malignancy (0.9%) were found. However, there was a high frequency of incidental findings such as disc protrusions (47%), renal and hepatic cysts/haemangioma (Figure 2). Critics highlight the high rate of indeterminate incidental and false-positive findings,<sup>29</sup> which can lead to unnecessary additional examinations and treatments, with potential negative psychological impact. Hence, any attempt at undertaking population-based screening should provide patients with appropriate counselling and advice, as well as clear pathways for managing incidental findings. A randomized trial with long-term follow-up is needed to establish whether WB-MRI for preventive health screening is beneficial.<sup>28</sup>

The complexity of dealing with incidental findings on WB-MRI is being explored, including within the German National Cohort (GNC).<sup>31</sup> The GNC is one of the largest population-based interdisciplinary and multi-centre cohort studies in Europe, involving 200,000 volunteers. The main goal is to investigate the development of common chronic diseases including cancer, diabetes, cardiovascular, neurodegenerative/psychiatric, respiratory, and infectious diseases. A subgroup of about 30,000 will undergo WB-MRI, of which about 3,000 participants are expected to reveal significant imaging finding or require additional evaluation.

#### Targeted or at-risk population screening

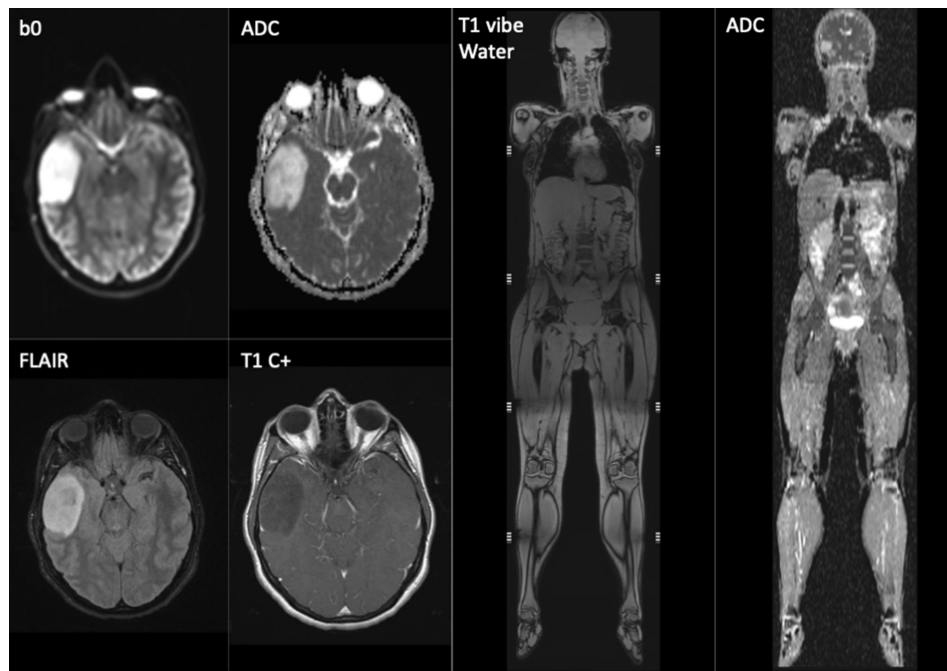
By contrast, targeted screening based on known high-risk genetic mutations such as TP53 mutation in Li-Fraumeni Syndrome (LFS) have reportedly a higher cancer detection rate of 9.1%.<sup>32</sup> International LFS experts are recommending annual WB-MRI for cancer detection in these patients in their 2017 guidelines.<sup>33</sup>

The SIGNIFY UK study,<sup>32</sup> included 88 participants, with 44 carriers of TP53 mutations and 44 matched healthy population controls. Four of the five identified malignancies were treated with curative intent (Figure 3). Similar findings were reported by Ballinger et al<sup>3</sup> in a meta-analysis that included 578 participants from 13 cohorts in six countries and reported 42 cancers in 39 individuals, with 35 new localized cancers treated with curative intent. The overall estimated detection rate for new, localized primary cancers was 7% (95% CI, 5–9%). The authors concluded that baseline WB-MRI in TP53 germline mutation carriers may form an integral part of management in this high-risk population. The conclusion is strengthened by Villani et al.<sup>34</sup> in a prospective, 11 years, observational study with biochemical and imaging surveillance in germline TP53 mutation carriers with LFS. The authors reported a 5-year overall survival of 88.8% (95% CI 78.7–100) in the surveillance group and 59.6% (47.2–75.2) in the non-surveillance group ( $p = 0.013$ ).

#### Childhood cancer predispositions syndromes

With advances in genetic testing, more families and children are being diagnosed with cancer predisposition syndromes. Up to 39% of childhood malignancy present with diagnostic or relevant mutations on whole-exome sequencing.<sup>35</sup> A survey by the Society for Paediatric Radiology in North America in 2018 reported 75% of the respondents using WB-MRI for cancer predisposition syndrome screening; majority (93%) of WB-MRI being performed in an academic institution, as a relatively recent trend in the last 6 years.<sup>36</sup> WB-MRI is gaining widespread recognition and support as an essential non-invasive, radiation-free diagnostic tool from paediatric oncologists, geneticists and families. The AACR Paediatric Working Group has recommended WB-MRI for several childhood cancer predisposition syndromes including LFS, neurofibromatosis Type 1 and Type 2 and schwannomatosis, hereditary retinoblastoma, constitutional mismatch repair deficiency syndrome and hereditary paraganglioma pheochromocytoma syndrome.<sup>37</sup>

Figure 3. Screening whole-body MRI in a 33-year-old female with p53 cancer predisposition syndrome. MRI of the brain including T1W post-contrast examination shows an asymptomatic right temporal lobe low-grade glioma, which was treated by curative surgery.



### WB-MRI IN ONCOLOGY

In the symptomatic adult population, WB-MRI has found particular application for the evaluation of malignant bone marrow disease (*e.g.*, myeloma and metastatic bone disease), while additionally offering information about soft tissue disease. Metastatic disease confined to be bone marrow is poorly evaluated by conventional imaging; bone sclerotic lesions with no soft tissue component are considered non-evaluable by RECIST 1.1<sup>38</sup> as osteoblastic response or osteoblastic progression could look similar on CT or morphological MRI. WB-MRI has also been applied to evaluate nodal disease in patients with lymphoma. More recently, WB-MRI has been prospectively evaluated as a “one-stop” imaging test for the initial cancer staging of a few common cancers (*e.g.*, lung and colon).

#### Multiple Myeloma

Multiple myeloma (MM) is a haematological disorder characterized by the accumulation of malignant plasma cells in the bone marrow. Bone involvement is one example of possible end organ damage, resulting in osteolysis, fractures and related morbidity and mortality. Focal marrow lesions on MRI are associated with inferior outcomes<sup>39</sup> and a positive MRI (>1 focal lesion of >5 mm) (Figure 4) is considered as an indication for treatment. WB-MRI is now included in recommendations from the International Myeloma Working Group,<sup>40</sup> and the National Institute for Clinical Excellence<sup>41</sup> at diagnosis and relapse. WB-MRI has superior sensitivity and interobserver agreement compared with other imaging techniques such as radiographs, CT and FDG PET/CT and sensitivity is improved by inclusion of DWI.<sup>16</sup> WB-MRI provides an opportunity for early diagnosis which leads to improved survival and quality of life.<sup>41</sup> Although the cost of WB-MRI is greater than CT, the net monetary benefits are

roughly equivalent because of the longer term benefits afforded by earlier diagnosis.<sup>41</sup>

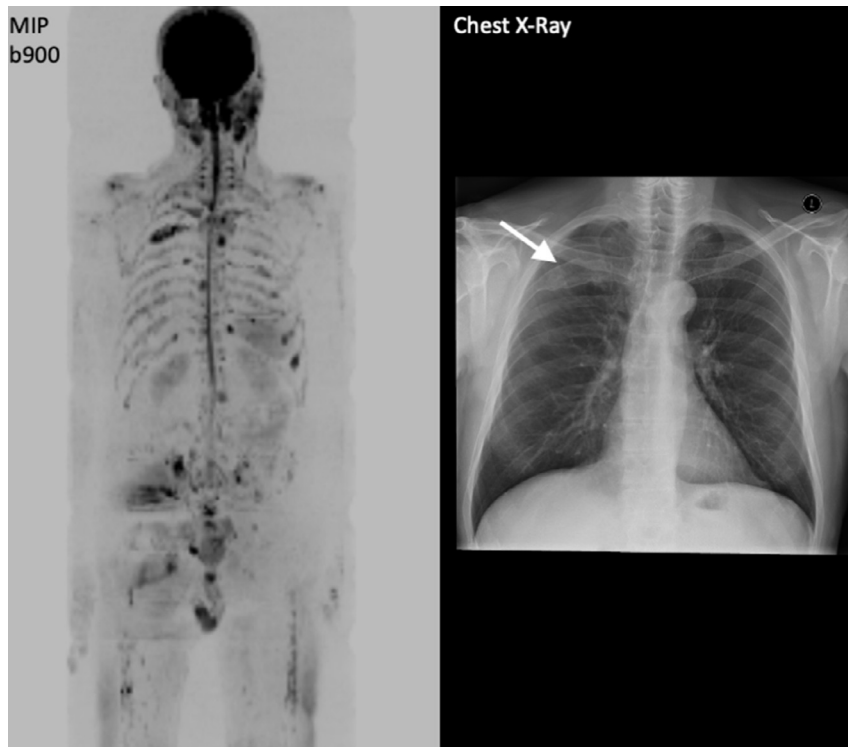
WB-MRI is also recommended for patients with suspected relapse and for monitoring response of non-secretory and oligosecretory myeloma.<sup>41,42</sup> The recently published Myeloma Response Assessment and Diagnosis System, or MY-RADS,<sup>8</sup> proposed standardised clinical acquisition and reporting protocols for WB-MRI including DWI and T1W-Dixon sequences, which can be performed on all major clinical MRI systems. The quantitative capabilities of DWI and T1W-Dixon are likely to increase their utility for response assessment.<sup>19,43</sup> Despite recommendations, WB-MRI adoption within the clinical community has been slow, due to a combination of factors including shortage of radiologists, lack of radiological expertise and scanner capacity in the wider community, which needs to be addressed. Enhanced software tools which can facilitate or accelerate image reading would also be welcomed.

#### Prostate cancer

As with other cancers, the presence, volume and distribution of metastatic disease in prostate cancer affects prognosis and therapy choices. The bone is the dominant site for metastatic disease in prostate cancer, with more than 50% of having bone-only metastases.<sup>10</sup>

At initial diagnosis, a local bi/multi-parametric MRI of the prostate could be combined with a WB-MRI as a “one-stop shop” for local and distant tumour staging for patients at high-risk for metastatic disease.<sup>44,45</sup> Like CT, MRI has modest diagnostic accuracy for nodal evaluation,<sup>46</sup> but has high accuracy for detecting bone metastases compared with bone scintigraphy. A

Figure 4. A 51-year-old male with solitary infiltration of the posterior third rib on skeletal survey led to discussion of local radiotherapy as primary treatment. 3D b900 inverse grey scale MIP from WB-MRI confirmed multifocal disease, resulting in a change to system treatment.



meta-analysis of 1102 metastatic prostate cancer patients found WB-MRI to be more sensitive (97%) than choline PET/CT (91%) and bone scintigraphy (78%) for detecting skeletal metastases.<sup>47</sup>

In advanced prostate cancer, WB-MRI can be used for assessing treatment response in bone, nodal and visceral metastases, and potential complications such as malignant spinal cord

compression, pathological fractures, hydronephrosis or local complications.<sup>48</sup> WB-MRI is not confounded by the “flare response”<sup>49</sup> encountered on bone scintigraphy (Figure 5) or prostate-specific membrane antigen (PSMA) PET, and is not modulated by androgen deprivation therapies, as is the case with PSMA PET.<sup>50</sup>

Figure 5. <sup>99m</sup>Tc-MDP Bone scan and WB-MRI images in a 60-year-old male with metastatic castrate resistant prostate carcinoma (mCRPC) illustrating the FLARE phenomenon. Bone scan performed in April 2018 after 12 weeks of chemotherapy showed several new bone lesions e.g. at T11 (arrows). Contemporaneous WB-MRI shows response with significant increase in ADC values (40%) of the lesion at T11 that appears “new” on bone scan. Note that the apparent new bone lesions on April 2018 in the lower thoracic spine bone scan were visible on the MRI from Jan 2018, but were occult/non-visible on the bone scan from Jan 2018.

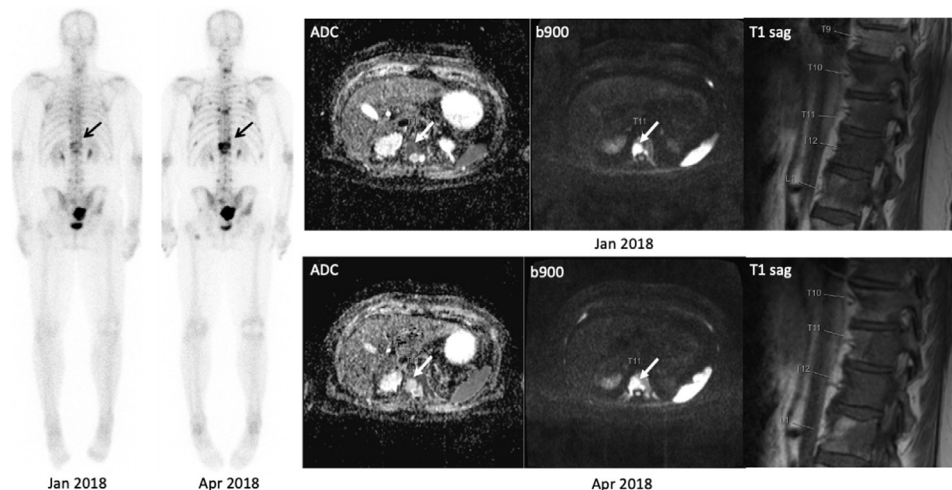
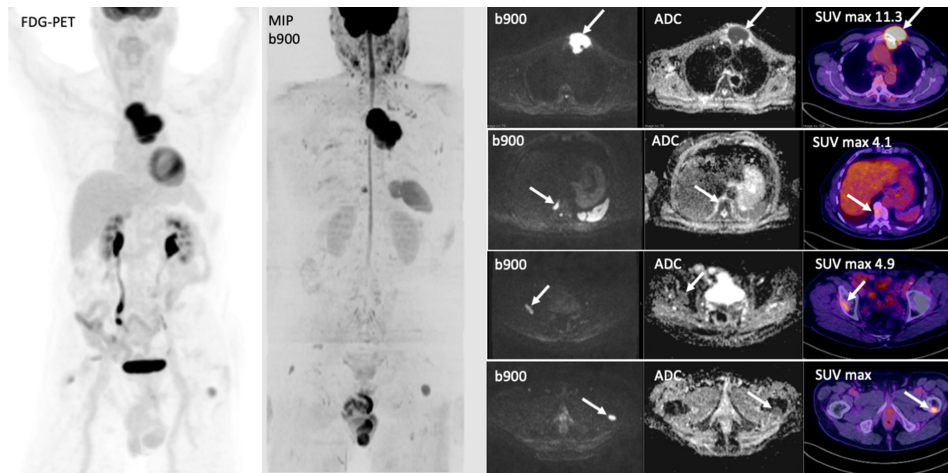


Figure 6. Coronal 3D MIP and axial, DWI and FDG-PET images show bone marrow involvement in a 80-year-old male with large B-cell lymphoma. The initial PET staging was reported as Stage 1 AE with a dominant sternal mass (a) and no other lesions. WB-MRI highlighted other focal bone lesions within T10 vertebral body (b), right acetabulum (c) and left femur (d) that were classified as inflammatory on PET imaging in view of the lower SUV values and their location adjacent to osteophytes and degenerative change. Following, tumour board discussion, the disease stage was changed to IVAE and treatment altered.



The METastasis Reporting and Data System for Prostate Cancer (MET-RADS-P)<sup>9</sup> recommends the minimum image acquisition, interpretation and reporting of WB-MRI in prostate cancer. The MET-RADS-P criteria combine the principles of prostate cancer working group (PCWG) criteria and RECIST 1.1<sup>51</sup> together with DWI criteria for bone metastases. The following prostate cancer patients appear to benefit most from WB-MRI: (1) newly diagnosed clinically high-risk/locally advanced patients in whom conventional imaging is equivocal; (2) non-metastatic (on conventional imaging) patients where the detection of metastatic disease would promote focal therapy (oligo-metastases) or systemic therapy (poly-metastases); (3) metastatic disease with predominant/only bone involvement; (4) metastatic disease with discordance between clinical findings, PSA values (especially low PSA secretors) and conventional imaging.<sup>48,52,53</sup>

### Breast cancer

In breast cancer, metastases to the<sup>54</sup> bone, lung and liver are common and usually assessed by CT. As in prostate cancer, WB-MRI is useful for patients with predominant bone disease. In addition, treatment of liver metastases can lead to liver pseudocirrhosis in upto 55%,<sup>55</sup> making the disease difficult to evaluate on CT. Furthermore, WB-MRI can also improve the detection of CT occult peritoneal disease. The addition of WB-MRI to conventional CT alters the treatment decisions in patients with metastatic breast cancer as WB-MRI can diagnose progressive bone/liver disease or partial response of bone disease (often reported stable on CT)<sup>56,57</sup> (Figure 6).

In breast cancer, WB-MRI seems most useful for<sup>1</sup>: high-risk presentation (inoperable locally advanced breast cancer, inflammatory and lobular histology cancers, heavy node positive disease) or pregnant females<sup>2</sup>; triple negative or HER2+ patients after adjuvant treatment with changing tumour biomarkers kinetics (CA 15-3 & CA 125)<sup>3,58</sup> for oligometastatic disease detection in patients considered for metastasis directed therapy;

4) assessing response for cutaneous or locally infiltrative disease-where CT can be inaccurate; 5) assessing response in bone only or bone & infiltrative liver disease especially in the presence of extensive liver fibrosis (regenerative nodular hyperplasia/pseudocirrhosis).

### Lymphoma

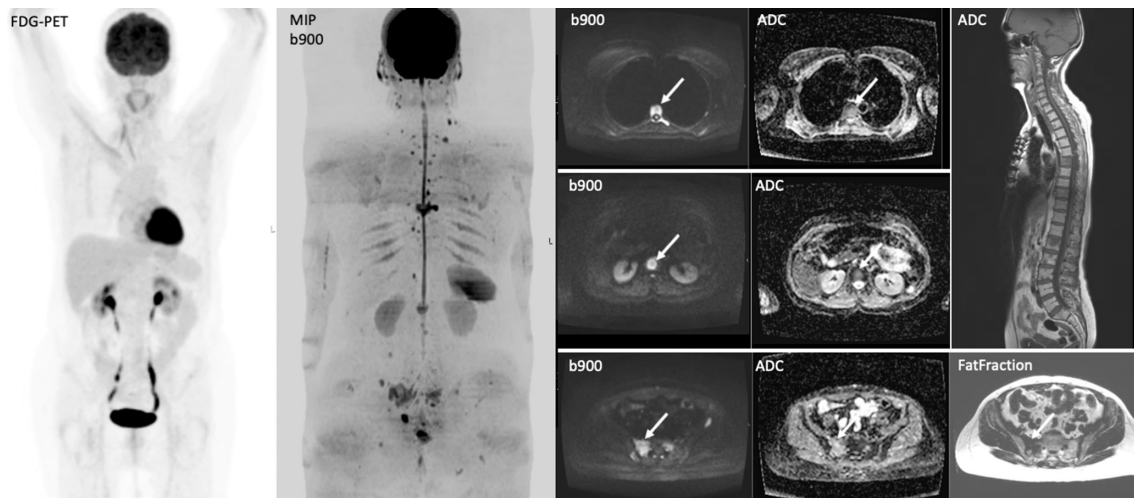
Several studies have shown that WB-MRI using DWI has similar accuracy to FDG-PET CT for staging FDG-avid lymphomas<sup>59,60</sup> and may have better sensitivity (94.4%) than FDG-PET/CT (60.9%) and contrast-enhanced CT (70.7%) in subtypes with variable FDG avidity.<sup>61</sup>

Emerging data highlight ADC as a potential response biomarker. In a study of non-Hodgkin lymphoma, the ADC value differentiated responders from non-responder for nodal/extra nodal disease with a high negative and positive predictive values.<sup>62</sup> WB-MRI assessment was less histology-dependent than FDG-PET/CT and thus may be complementary to PET for reducing radiation exposure in young patients, especially in those who did not receive radiotherapy as part of their treatment. Current data also support WB-MRI for lymphoma surveillance, in lymphomas with variable/low FDG avidity and non-follicular indolent lymphomas<sup>63,64</sup> (Figure 7).

### Melanoma

A recent European consensus recommended whole-body examinations with CT or PET-CT in combination with brain MRI for stage IIIB of higher disease.<sup>65</sup> Meta-analysis and systematic review have found evidence for WB-MRI as an alternative to PET/CT.<sup>66,67</sup> A recent study showed that non-enhanced WB-MRI with DWI is promising for detecting melanoma extracranial metastases.<sup>68</sup> More recently, Pflugfelder *et al*, on behalf of the German Dermatologic Society and the Dermatologic Cooperative Oncology Group, recommend WB-MR for imaging advanced melanoma (stage III or higher), stating

Figure 7. A 65-year-old female with history of right invasive lobular breast carcinoma presenting with raised tumour marker CA15-345 U/ml and back pain. The tumour showed lymphovascular invasion; with ER8 PRO Her-2 negative. WB-MRI show multiple vertebral and pelvic bone metastases that were occult on PET-CT without FDG tracer uptake.



the equivalence of WB-MRI compared with CT and PET/CT. WB-MRI recommends the follow-up of patients with staged IIC to IV melanoma.<sup>69</sup>

#### Ovarian cancer

The most important prognostic factor in ovarian cancer is complete tumour resection at presentation or interval debulking surgery.<sup>70</sup> The performance of WB-MRI with DWI is similar to FDG PET-CT for detecting retroperitoneal lymphadenopathy/distant metastases but WB-MRI has higher sensitivity than CT and FDG-PET/CT for peritoneal staging, mesenteric root infiltration and bowel wall involvement by peritoneal carcinomatosis,<sup>71-73</sup> which better predicts the eligibility and success of surgery.

#### WB-MRI as a single modality compared with standard multi-modality cancer imaging assessments

Recently, the STREAMLINE Investigators published the results of two, UK multicentre studies (16 hospitals) comparing WB-MRI with standard NICE-approved diagnostic pathways for staging colorectal cancer<sup>4</sup> and non-small cell lung cancer<sup>5</sup> using WB-MRI as the initial staging test showed similar accuracy to standard pathways, but was associated with reduced staging time and costs.

The STREAMLINE C trial recruited 370 patients with newly diagnosed colorectal cancer, 299 of whom completed the trial. Pathway sensitivity was 67% for WB-MRI and 63% for standard pathways. Specificity did not differ between WB-MRI (95%) and standard pathways (93%). Agreement with the multidisciplinary team's final treatment decision was 96% for WB-MRI and 95% for the standard pathway. Time to complete staging was shorter for WB-MRI (median, 8 days) than for the standard pathway (13 days). The mean per-patient staging costs were £216 for WB-MRI and £285 for standard pathways.

The STREAMLINE L recruited 353 patients newly diagnosed NSCLC that was potentially radically treatable on diagnostic chest CT (defined as stage IIIb or less), 187 of whom completed the trial; 52 (28%) had metastasis at baseline. Pathway sensitivity was 50% for WB-MRI and 54% for standard pathways. Specificity did not differ between WB-MRI (93%) and standard pathways (95% [91-98])(Figure 8)). Agreement with the multidisciplinary team's final treatment decision was 98% for WB-MRI and 99% for the standard pathway. Median time to complete staging was shorter for WB-MRI (13 days) than for the standard pathway (19 days). Mean per-patient costs were £317 for WBI-MRI and £620 for standard pathway.

#### WB-MRI IN NON-ONCOLOGICAL APPLICATIONS

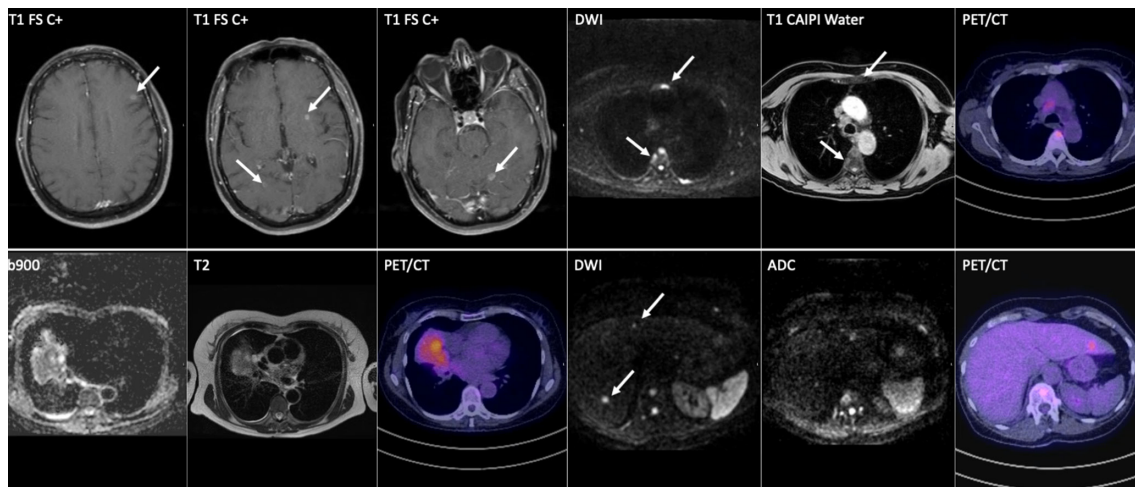
##### Inflammatory joint disorders

MRI is the examination of choice for detecting early inflammatory changes such as bone marrow oedema, disks enthesitis, and synovitis, as well as structural changes such as erosions, new bone formation, ankylosis and fractures. MRI can also often provide soft tissue information such as muscle, cutaneous/subcutaneous tissue, viscera and nodal involvement. The Spondylo-arthritis International Society classification criteria for axial spondylarthritis (SpA) consider MRI to be of choice for detecting active inflammation in the subchondral bone underlying the sacroiliac joints.<sup>74</sup>

WB-MRI enables global assessment of active and chronic inflammatory changes in the axial and peripheral skeleton.<sup>12,75,76</sup>

Consequently, there has been an increased interest in using WB-MRI for the comprehensive examination of systemic inflammatory/infective disorders, including but not limited to spondyloarthropathies, myopathies, sarcoidosis, Langerhans cell histiocytosis, chronic osteomyelitis or genetic disorders such as Hereditary Multiple Exostoses and metabolic storage disorders.

Figure 8. A 60-year-old male with lung adenocarcinoma. FDG PET-CT and WB-MRI demonstrate liver, bone and brain metastases, which were not visible on the staging CT (not shown). White arrows show concordant lesions detected by both FDG PET-CT and WB-MRI. However, WB-MRI showed additional liver and bone lesions (grey arrows), while post-contrast T1W brain images show cerebral metastases not visible on FDG PET-CT (not shown).



To standardise assessment, the MRI Whole-Body Score for Inflammation in Peripheral Joints and Enteses in Inflammatory Arthritis (MRI-WIPE) scoring system was published in 2019.<sup>27</sup> MRI-WIPE scoring documents separate the inflammation in joints (arthritis) and at enteses (enthesitis) for soft tissues (synovitis at joints, soft tissue inflammation at enteses) and bone (osteitis). Synovitis and soft tissue inflammation are to be assessed on T1-post-Gd images and osteitis predominantly on STIR/T2Wfat-suppressed images. Each component is scored on a semi-quantitative scale of 0–3 (none/mild/moderate/severe).<sup>27,77,78</sup> In total, 83 peripheral joints and 33 enteses are assessed by adding all scores together, the total range is 0–738 (joints 0–537; enteses 0–201). MRI-WIPE reading time was estimated to be  $\leq 60$  min. However, MRI-WIPE scores are semi-quantitative and have significant interobserver variability.<sup>27,79</sup> The MRI-WIPE score was more reliable when averaged over two or three readers: the reported ICC (interclass correlation coefficient) of MRI-WIPE was 0.28 (–0.37–0.92) by one reader compared with 0.67 (0.30–0.87) for four readers.<sup>27</sup> Even with these limitations, the MRI total inflammation index has been successfully applied in clinical trials.<sup>80–82</sup>

Recently, DWI was shown to be more sensitive than STIR<sup>12,83</sup> and faster to acquire.<sup>84</sup> Together with T1W/T2W T1W-Dixon sequences, these should pave the way for quantitative assessment of bone marrow oedema and inflammation using parameters such as ADC<sup>12,85,86</sup> and T1W-Dixon derived fat fractions.<sup>87</sup>

### Osteomyelitis

Chronic recurrent multifocal osteomyelitis is a non-bacterial osteomyelitis in children and adolescents.<sup>88</sup> WB-MRI is a valuable tool to assess the disease extent and for disease surveillance. A small retrospective study using WB-MRI identified two main diagnostic phenotypic: the “tibio-appendicular multifocal” (>50%) pattern and the “claviculo-spinal paucifocal” (24%) pattern.<sup>89</sup>

### Gaucher disease

Gaucher disease is the most prevalent lysosomal storage disorder caused by lysosomal  $\beta$ -glucocerebrosidase deficiency, which leads to the accumulation of glucocerebroside in the bone marrow, liver, and spleen. In the skeleton, osteopenia and focal osseous lesions, such as bone infarctions, avascular necrosis, or osteolysis, are observed, as well as long bone deformities (*e.g.*, Erlenmeyer flask deformities). WB-MRI is used to assess disease severity and several WB-MRI-based scores have been described based on T1W-Dixon quantitative chemical shift MRI.<sup>90</sup> WB-MRI can be used to monitor the response to enzyme replacement therapy<sup>91</sup> as well as skeletal and visceral complications.

### Familial lipodystrophy syndromes

Lipodystrophies are systemic disorders characterized by loss of adipose tissue at some anatomic sites, frequently accompanied by fat accumulation in ectopic sites, such as in the liver and muscle.<sup>92</sup> WB-MRI allows an accurate depiction of the abnormal fat loss, as well as ectopic fat deposition.

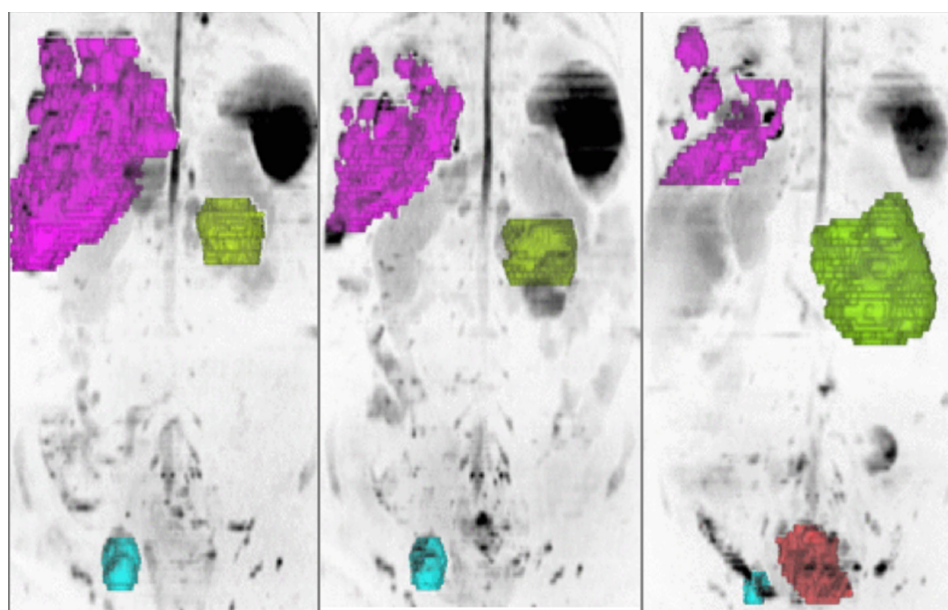
### Other emerging indications

WB-MRI is being evaluated in suspected child abuse to assess the integrity of the entire skeleton, brain and intra-abdominal viscera.<sup>93</sup> WB-MRI is also being applied to characterize anorexia nervosa-induced marrow changes that may correlate with disease severity.<sup>94</sup> Last but not least, WB-MRI offers excellent anatomical detail and characterization of the brain, heart and abdominal organs for post-mortem examinations, and can detect bone injury not visible on post-mortem CT. MRI can also distinguish between post-mortem and ante-mortem fractures, and is being utilised in forensic radiology.<sup>95</sup>

### Summary and future developments

In 2016, the UK quantitative WB-DWI technical workgroup was established to provide technical guidelines, with the aim to maximise the accuracy and reproducibility of WB-DWI quantitative

Figure 9. 3D MIP inverted b900 images in a 47-year-old female with advanced ovarian cancer. The different tumour sites are colour-coded according to the organ involved liver metastases (pink), peritoneal disease (green), pelvic lymphadenopathy (blue) and local relapse (orange). Pre- and post-chemotherapy images show response heterogeneity with decrease in the liver and nodal disease, but increase in peritoneal and local disease.



parameters.<sup>26</sup> The workgroup provided detailed acquisition parameters, optimization procedures and quality assurance when setting up WB-DWI, both at 3T and 1.5T for routine clinical use and multicentre trials, recognising that quantitative WB-MRI will become increasingly important.

Disease specific guidelines are emerging, such as MET-RADS-P<sup>9</sup> and MY-RADS,<sup>8</sup> with recommendations for image acquisition and quantitative data analysis. For ADC quantification, a minimum of two diffusion-weightings (b-values) are necessary, with the lower b-value between 50 and 100 s/mm<sup>2</sup> (to suppress vascular perfusion effects) and the higher b-value between 800 and 1000 s/mm<sup>2</sup>. The use of three b-values with the additional b-value in the range of 500 to 600 s/mm<sup>2</sup> is recommended for optimal ADC quantification before and after treatment. The ADC can be calculated at each lesion level (subjective choice of representative lesions in a manner similar to RECIST1.1) or at the whole body level – global ADC (gADC) across all lesions; the latter is time-consuming requiring manual or semi-automated tumour segmentation. Another quantitative WB-MRI parameter, total diffusion volume (tDV), is based whole-body tumour segmentation to summate all the disease volume. In addition, T1W-Dixon technique derived fat fraction is emerging as a potential biomarker, especially for bone marrow disease in myeloma.<sup>87</sup>

While the repeatability of ADC measurement is well characterised as around 10%,<sup>96</sup> there is still limited data with regard to the percentage change in WB-MRI parameters (ADC and tDV) associated with clinically significant tumour response. In a study<sup>97</sup>

correlating histological parameters and ADC measurements in patients with prostate bone metastases, bone biopsies revealed that areas that contained tumour cells had a significantly lower ADC compared with areas that showed no detectable tumour ( $0.898 \times 10^3$  mm<sup>2</sup>/s vs  $1.617 \times 10^3$  mm<sup>2</sup>/s;  $p < .001$ ). The use of an ADC threshold ( $1.5\text{--}1.6 \times 10^{-3}$  mm<sup>2</sup>/s)<sup>9</sup> above which represents treated disease<sup>98</sup> has been proposed but requires further validation.

Undoubtedly, the indications for WB-MRI will continue to expand. Patients and clinicians are willing to trade attributes, such as faster diagnosis, improvements in diagnostic accuracy, reducing radiation exposure and the need for i.v. contrast, against the longer examination time of WB-MRI scan. Recent developments using ultra-short TE (UTE) MRI and compressed-sensing sequences are likely to improve lung metastasis detection using WB-MRI to provide a more comprehensive evaluation.

Future technological developments including the use AI to substantially reduce the WB-DWI acquisition time<sup>99</sup> so that the technique can be performed in less than 10 min and be widely generalised across different vendor platforms and disease settings. By combining high spatial anatomical resolution with functional imaging (DWI), WB-MRI can also depict intra- and interlesional heterogeneity (Figure 9), paving the way to a better understanding of treatment effects in advanced disease.<sup>100</sup> Hybrid imaging combining WB-MRI with modern radionuclear tracers will allow a better characterisation of disease at staging and throughout the treatment pathways, by harnessing the synergies of these modern imaging techniques.

## REFERENCES

- Lam DL, Larson DB, Eisenberg JD, Forman HP, Lee CI. Communicating potential radiation-induced cancer risks from medical imaging directly to patients. *AJR Am J Roentgenol* 2015; **205**: 962–70. doi: <https://doi.org/10.2214/AJR.15.15057>
- Hendee WR, O'Connor MK. Radiation risks of medical imaging: separating fact from fantasy. *Radiology* 2012; **264**: 312–21. doi: <https://doi.org/10.1148/radiol.12112678>
- Ballinger ML, Best A, Mai PL, Khincha PP, Loud JT, Peters JA, et al. Baseline surveillance in Li-Fraumeni syndrome using whole-body magnetic resonance imaging: a meta-analysis. *JAMA Oncol* 2017; **3**: 1634–9. doi: <https://doi.org/10.1001/jamaoncol.2017.1968>
- Taylor SA, Mallett S, Beare S, Bhatnagar G, Blunt D, Boavida P, et al. Diagnostic accuracy of whole-body MRI versus standard imaging pathways for metastatic disease in newly diagnosed colorectal cancer: the prospective streamline C trial. *Lancet Gastroenterol Hepatol* 2019; **4**: 529–37. doi: [https://doi.org/10.1016/S2468-1253\(19\)30056-1](https://doi.org/10.1016/S2468-1253(19)30056-1)
- Taylor SA, Mallett S, Ball S, Beare S, Bhatnagar G, Bhowmik A, et al. Diagnostic accuracy of whole-body MRI versus standard imaging pathways for metastatic disease in newly diagnosed non-small-cell lung cancer: the prospective streamline L trial. *Lancet Respir Med* 2019; **7**: 523–32. doi: [https://doi.org/10.1016/S2213-2600\(19\)30090-6](https://doi.org/10.1016/S2213-2600(19)30090-6)
- Gottumukkala RV, Gee MS, Hampilos PJ, Greer M-LC. Current and emerging roles of whole-body MRI in evaluation of pediatric cancer patients. *Radiographics* 2019; **39**: 516–34. doi: <https://doi.org/10.1148/rg.2019180130>
- Han SN, Amant F, Michielsen K, De Keyzer F, Fieuws S, Van Calsteren K, et al. Feasibility of whole-body diffusion-weighted MRI for detection of primary tumour, nodal and distant metastases in women with cancer during pregnancy: a pilot study. *Eur Radiol* 2018; **28**: 1862–74. doi: <https://doi.org/10.1007/s00330-017-5126-z>
- Messiou C, Hillengass J, Delorme S, Lecouvet FE, Mouloupoulos LA, Collins DJ, et al. Guidelines for acquisition, interpretation, and reporting of whole-body MRI in myeloma: myeloma response assessment and diagnosis system (MY-RADS). *Radiology* 2019; **291**: 5–13. doi: <https://doi.org/10.1148/radiol.2019181949>
- Padhani AR, Lecouvet FE, Tunariu N, Koh D-M, De Keyzer F, Collins DJ, et al. Metastasis reporting and data system for prostate cancer: practical guidelines for acquisition, interpretation, and reporting of whole-body magnetic resonance imaging-based evaluations of multiorgan involvement in advanced prostate cancer. *Eur Urol* 2017; **71**: 81–92. doi: <https://doi.org/10.1016/j.eururo.2016.05.033>
- Padhani AR, Lecouvet FE, Tunariu N, Koh D-M, De Keyzer F, Collins DJ, et al. Rationale for Modernising imaging in advanced prostate cancer. *Eur Urol Focus* 2017; **3**(2-3): 223–39. doi: <https://doi.org/10.1016/j.euf.2016.06.018>
- Petralia G, Padhani AR, Pricolo P, Zugni F, Martinetti M, Summers PE, et al. Whole-Body magnetic resonance imaging (WB-MRI) in oncology: recommendations and key uses. *Radiol Med* 2019; **124**: 218–33. doi: <https://doi.org/10.1007/s11547-018-0955-7>
- Barakat E, Kirchgessner T, Triqueneaux P, Galant C, Stoenoiu M, Lecouvet FE. Whole-Body magnetic resonance imaging in rheumatic and systemic diseases: from emerging to validated indications. *Magn Reson Imaging Clin N Am* 2018; **26**: 581–97. doi: <https://doi.org/10.1016/j.mric.2018.06.005>
- Elessawy SS, Abdelsalam EM, Abdel Razek E, Tharwat S. Whole-Body MRI for full assessment and characterization of diffuse inflammatory myopathy. *Acta Radiol Open* 2016; **5**: 205846011666821. doi: <https://doi.org/10.1177/2058460116668216>
- Morone M, Bali MA, Tunariu N, Messiou C, Blackledge M, Grazioli L, et al. Whole-Body MRI: current applications in oncology. *AJR Am J Roentgenol* 2017; **209**: W336–49. doi: <https://doi.org/10.2214/AJR.17.17984>
- Tomas X, Milisenda JC, Garcia-Diez AI, Prieto-Gonzalez S, Faruch M, Pomes J, et al. Whole-Body MRI and pathological findings in adult patients with myopathies. *Skeletal Radiol* 2019; **48**: 653–76. doi: <https://doi.org/10.1007/s00256-018-3107-1>
- Pearce T, Philip S, Brown J, Koh DM, Burn PR. Bone metastases from prostate, breast and multiple myeloma: differences in lesion conspicuity at short-tau inversion recovery and diffusion-weighted MRI. *Br J Radiol* 2012; **85**: 1102–6. doi: <https://doi.org/10.1259/bjr/30649204>
- Faruch M, Garcia AI, Del Amo M, Pomes J, Isern J, González SP, et al. Diffusion-Weighted magnetic resonance imaging is useful for assessing inflammatory myopathies. *Muscle Nerve* 2019; **59**: 555–60. doi: <https://doi.org/10.1002/mus.26438>
- <https://www.fda.gov/drugs/drug-safety-and-availability/fda-drug-safety-communication-fda-warns-gadolinium-based-contrast-agents-gbcas-are-retained-body>
- Latifoltojar A, Hall-Craggs M, Bainbridge A, Rabin N, Popat R, Rismani A, et al. Whole-Body MRI quantitative biomarkers are associated significantly with treatment response in patients with newly diagnosed symptomatic multiple myeloma following bortezomib induction. *Eur Radiol* 2017; **27**: 5325–36. doi: <https://doi.org/10.1007/s00330-017-4907-8>
- Mosavi F, Ullenhag G, Ahlström H. Whole-Body MRI including diffusion-weighted imaging compared to CT for staging of malignant melanoma. *Ups J Med Sci* 2013; **118**: 91–7. doi: <https://doi.org/10.3109/03009734.2013.778375>
- Koh D-M, Lee J-M, Bittencourt LK, Blackledge M, Collins DJ. Body diffusion-weighted MR imaging in oncology: imaging at 3 T. *Magn Reson Imaging Clin N Am* 2016; **24**: 31–44. doi: <https://doi.org/10.1016/j.mric.2015.08.007>
- McGuirt D. Alternatives to sedation and general anesthesia in pediatric magnetic resonance imaging: a literature review. *Radiol Technol* 2016; **88**: 18–26.
- Miles A, Taylor SA, Evans REC, Halligan S, Beare S, Bridgewater J, et al. Patient preferences for whole-body MRI or conventional staging pathways in lung and colorectal cancer: a discrete choice experiment. *Eur Radiol* 2019; **29**: 3889–900. doi: <https://doi.org/10.1007/s00330-019-06153-4>
- Oliveri S, Pricolo P, Pizzoli S, Faccio F, Lampis V, Summers P, et al. Investigating cancer patient acceptance of whole body MRI. *Clin Imaging* 2018; **52**: 246–51. doi: <https://doi.org/10.1016/j.clinimag.2018.08.004>
- Adams HJA, Kwee TC, Vermoolen MA, Ludwig I, Bierings MB, Nievelstein RAJ, et al. Whole-Body MRI vs. CT for staging lymphoma: patient experience. *Eur J Radiol* 2014; **83**: 163–6. doi: <https://doi.org/10.1016/j.ejrad.2013.10.008>
- Barnes A, Alonzi R, Blackledge M, Charles-Edwards G, Collins DJ, Cook G, et al. Uk quantitative WB-DWI technical Workgroup: consensus meeting recommendations on optimisation, quality control, processing and analysis of quantitative whole-body diffusion-weighted imaging for cancer. *Br J Radiol* 2018; **91**:

20170577. doi: <https://doi.org/10.1259/bjr.20170577>
27. Krabbe S, Eshed I, Gandjbakhch F, Pedersen SJ, Bird P, Mathew AJ, et al. Development and validation of an OMERACT MRI whole-body score for inflammation in peripheral joints and Enteses in inflammatory arthritis (MRI-WIPE). *J Rheumatol* 2019; **46**: 1215–21. doi: <https://doi.org/10.3899/jrheum.181084>
  28. Kwee RM, Kwee TC. Whole-Body MRI for preventive health screening: a systematic review of the literature. *J Magn Reson Imaging* 2019; **50**: 1489–503. doi: <https://doi.org/10.1002/jmri.26736>
  29. Hegenscheid K, Seipel R, Schmidt CO, Völzke H, Kühn J-P, Biffar R, et al. Potentially relevant incidental findings on research whole-body MRI in the general adult population: frequencies and management. *Eur Radiol* 2013; **23**: 816–26. doi: <https://doi.org/10.1007/s00330-012-2636-6>
  30. Lee SY, Park HJ, Kim MS, Rho MH, Han CH. An initial experience with the use of whole body MRI for cancer screening and regular health checks. *PLoS One* 2018; **13**: e0206681. doi: <https://doi.org/10.1371/journal.pone.0206681>
  31. Hegedüs P, von Stackelberg O, Neumann C, Selder S, Werner N, Erdmann P, et al. How to report incidental findings from population whole-body MRI: view of participants of the German national cohort. *Eur Radiol* 2019; **29**: 5873–8. doi: <https://doi.org/10.1007/s00330-019-06077-z>
  32. Saya S, Killick E, Thomas S, Taylor N, Bancroft EK, Rothwell J, et al. Baseline results from the UK signify study: a whole-body MRI screening study in TP53 mutation carriers and matched controls. *Fam Cancer* 2017; **16**: 433–40. doi: <https://doi.org/10.1007/s10689-017-9965-1>
  33. Kratz CP, Achatz MI, Brugières L, Frebourg T, Garber JE, Greer M-LC, et al. Cancer screening recommendations for individuals with Li-Fraumeni syndrome. *Clin Cancer Res* 2017; **23**: e38–45. doi: <https://doi.org/10.1158/1078-0432.CCR-17-0408>
  34. Villani A, Shore A, Wasserman JD, Stephens D, Kim RH, Druker H, et al. Biochemical and imaging surveillance in germline TP53 mutation carriers with Li-Fraumeni syndrome: 11 year follow-up of a prospective observational study. *Lancet Oncol* 2016; **17**: 1295–305. doi: [https://doi.org/10.1016/S1470-2045\(16\)30249-2](https://doi.org/10.1016/S1470-2045(16)30249-2)
  35. Saade-Lemus S, Degnan AJ, Acord MR, Srinivasan AS, Reid JR, Servaes SE, et al. Whole-Body magnetic resonance imaging of pediatric cancer predisposition syndromes: special considerations, challenges and perspective. *Pediatr Radiol* 2019; **49**: 1506–15. doi: <https://doi.org/10.1007/s00247-019-04431-3>
  36. Schooler GR, Davis JT, Daldrup-Link HE, Frush DP. Current utilization and procedural practices in pediatric whole-body MRI. *Pediatr Radiol* 2018; **48**: 1101–7. doi: <https://doi.org/10.1007/s00247-018-4145-5>
  37. Greer M-LC, Voss SD, States LJ. Pediatric cancer predisposition imaging: focus on whole-body MRI. *Clin Cancer Res* 2017; **23**: e6–13. doi: <https://doi.org/10.1158/1078-0432.CCR-17-0515>
  38. Schwartz LH, Seymour L, Litière S, Ford R, Gwyther S, Mandrekas S, et al. RECIST 1.1 - Standardisation and disease-specific adaptations: Perspectives from the RECIST Working Group. *Eur J Cancer* 2016; **62**: 138–45. doi: <https://doi.org/10.1016/j.ejca.2016.03.082>
  39. Hillengass J, Fechtner K, Weber M-A, Bäuerle T, Ayyaz S, Heiss C, et al. Prognostic significance of focal lesions in whole-body magnetic resonance imaging in patients with asymptomatic multiple myeloma. *J Clin Oncol* 2010; **28**: 1606–10. doi: <https://doi.org/10.1200/JCO.2009.25.5356>
  40. Rajkumar SV, Dimopoulos MA, Palumbo A, Blade J, Merlini G, Mateos M-V, et al. International myeloma Working group updated criteria for the diagnosis of multiple myeloma. *Lancet Oncol* 2014; **15**: e538–48. doi: [https://doi.org/10.1016/S1470-2045\(14\)70442-5](https://doi.org/10.1016/S1470-2045(14)70442-5)
  41. Overview | Myeloma: diagnosis and management | Guidance | NICE: NICE. 2020. Available from: <https://www.nice.org.uk/guidance/ng35>.
  42. Chantry A, Kazmi M, Barrington S, Goh V, Mulholland N, Streetly M, et al. Guidelines for the use of imaging in the management of patients with myeloma. *Br J Haematol* 2017; **178**: 380–93. doi: <https://doi.org/10.1111/bjh.14827>
  43. Giles SL, Messiou C, Collins DJ, Morgan VA, Simpkin CJ, West S, et al. Whole-Body diffusion-weighted MR imaging for assessment of treatment response in myeloma. *Radiology* 2014; **271**: 785–94. doi: <https://doi.org/10.1148/radiol.13131529>
  44. Trabulsi EJ, Rumble RB, Jadvar H, Hope T, Pomper M, Turkbey B, et al. Optimum imaging strategies for advanced prostate cancer: ASCO guideline. *J Clin Oncol* 2020; **JCO1902757**.
  45. Johnston EW, Latifoltojar A, Sidhu HS, Ramachandran N, Sokolska M, Bainbridge A, et al. Multiparametric whole-body 3.0-T MRI in newly diagnosed intermediate- and high-risk prostate cancer: diagnostic accuracy and interobserver agreement for nodal and metastatic staging. *Eur Radiol* 2019; **29**: 3159–69. doi: <https://doi.org/10.1007/s00330-018-5813-4>
  46. Lecouvet FE, El Mouedden J, Collette L, Coche E, Danse E, Jamar F, et al. Can whole-body magnetic resonance imaging with diffusion-weighted imaging replace Tc 99m bone scanning and computed tomography for single-step detection of metastases in patients with high-risk prostate cancer? *Eur Urol* 2012; **62**: 68–75. doi: <https://doi.org/10.1016/j.eururo.2012.02.020>
  47. Shen G, Deng H, Hu S, Jia Z. Comparison of choline-PET/CT, MRI, SPECT, and bone scintigraphy in the diagnosis of bone metastases in patients with prostate cancer: a meta-analysis. *Skeletal Radiol* 2014; **43**: 1503–13. doi: <https://doi.org/10.1007/s00256-014-1903-9>
  48. Gillessen S, Attard G, Beer TM, Beltran H, Bossi A, Bristow R, et al. Management of patients with advanced prostate cancer: the report of the advanced prostate cancer consensus conference APCCC 2017. *Eur Urol* 2018; **73**: 178–211. doi: <https://doi.org/10.1016/j.eururo.2017.06.002>
  49. Fanti S, Hadaschik B, Herrmann K. Proposal of systemic therapy response assessment criteria in time of PSMA PET/CT imaging: PSMA PET progression (ppp). *J Nucl Med* 2019;.
  50. Meller B, Bremmer F, Sahlmann CO, Hijazi S, Bouter C, Trojan L, et al. Alterations in androgen deprivation enhanced prostate-specific membrane antigen (PSMA) expression in prostate cancer cells as a target for diagnostics and therapy. *EJNMMI Res* 2015; **5**: 66. doi: <https://doi.org/10.1186/s13550-015-0145-8>
  51. Scher HI, Morris MJ, Stadler WM, Higano C, Basch E, Fizazi K, et al. Trial design and objectives for castration-resistant prostate cancer: updated recommendations from the prostate cancer clinical trials Working group 3. *J Clin Oncol* 2016; **34**: 1402–18. doi: <https://doi.org/10.1200/JCO.2015.64.2702>
  52. Bryce AH, Alumkal JJ, Armstrong A, Higano CS, Iversen P, Sternberg CN, et al. Radiographic progression with nonrising PSA in metastatic castration-resistant prostate cancer: post hoc analysis of prevail. *Prostate Cancer Prostatic Dis* 2017; **20**: 221–7. doi: <https://doi.org/10.1038/pcan.2016.71>
  53. Aparicio AM, Harzstark AL, Corn PG, Wen S, Araujo JC, Tu S-M, et al. Platinum-Based chemotherapy for variant castrate-resistant prostate cancer. *Clin Cancer Res* 2013; **19**:

- 3621–30. doi: <https://doi.org/10.1158/1078-0432.CCR-12-3791>
54. Steinauer K, Huang DJ, Eppenberger-Castori S, Amann E, Güth U. Bone metastases in breast cancer: frequency, metastatic pattern and non-systemic locoregional therapy. *J Bone Oncol* 2014; **3**: 54–60. doi: <https://doi.org/10.1016/j.jbo.2014.05.001>
  55. Oliai C, Douek ML, Rhoane C, Bhutada A, Ge PS, Runyon BA, et al. Clinical features of pseudocirrhosis in metastatic breast cancer. *Breast Cancer Res Treat* 2019; **177**: 409–17. doi: <https://doi.org/10.1007/s10549-019-05311-y>
  56. Kosmin M, Makris A, Joshi PV, Ah-See M-L, Woolf D, Padhani AR. The addition of whole-body magnetic resonance imaging to body computerised tomography alters treatment decisions in patients with metastatic breast cancer. *Eur J Cancer* 2017; **77**: 109–16. doi: <https://doi.org/10.1016/j.ejca.2017.03.001>
  57. Zugni F, Ruju F, Pricolo P, Alessi S, Iorfida M, Colleoni MA, et al. The added value of whole-body magnetic resonance imaging in the management of patients with advanced breast cancer. *PLoS One* 2018; **13**: e0205251. doi: <https://doi.org/10.1371/journal.pone.0205251>
  58. Di Gioia D, Stieber P, Schmidt GP, Nagel D, Heinemann V, Baur-Melnyk A. Early detection of metastatic disease in asymptomatic breast cancer patients with whole-body imaging and defined tumour marker increase. *Br J Cancer* 2015; **112**: 809–18. doi: <https://doi.org/10.1038/bjc.2015.8>
  59. Mayerhoefer ME, Karanikas G, Kletter K, Prosch H, Kiesewetter B, Skrabs C, et al. Evaluation of diffusion-weighted magnetic resonance imaging for follow-up and treatment response assessment of lymphoma: results of an 18F-FDG-PET/CT-Controlled prospective study in 64 patients. *Clin Cancer Res* 2015; **21**: 2506–13. doi: <https://doi.org/10.1158/1078-0432.CCR-14-2454>
  60. Stecco A, Buemi F, Iannesi A, Carriero A, Gallamini A. Current concepts in tumor imaging with whole-body MRI with diffusion imaging (WB-MRI-DWI) in multiple myeloma and lymphoma. *Leuk Lymphoma* 2018; **59**: 2546–56. doi: <https://doi.org/10.1080/10428194.2018.1434881>
  61. Mayerhoefer ME, Karanikas G, Kletter K, Prosch H, Kiesewetter B, Skrabs C, et al. Evaluation of diffusion-weighted MRI for pretherapeutic assessment and staging of lymphoma: results of a prospective study in 140 patients. *Clin Cancer Res* 2014; **20**: 2984–93. doi: <https://doi.org/10.1158/1078-0432.CCR-13-3355>
  62. De Paepe K, Bevernage C, De Keyzer F, Wolter P, Gheysens O, Janssens A, et al. Whole-Body diffusion-weighted magnetic resonance imaging at 3 tesla for early assessment of treatment response in non-Hodgkin lymphoma: a pilot study. *Cancer Imaging* 2013; **13**: 53–62. doi: <https://doi.org/10.1102/1470-7330.2013.0006>
  63. Galia M, Albano D, Tarella C, Patti C, Sconfienza LM, Mulè A, et al. Whole body magnetic resonance in indolent lymphomas under watchful waiting: the time is now. *Eur Radiol* 2018; **28**: 1187–93. doi: <https://doi.org/10.1007/s00330-017-5071-x>
  64. Albano D, Bruno A, Patti C, Micci G, Midiri M, Tarella C, et al. Whole-Body magnetic resonance imaging (WB-MRI) in lymphoma: state of the art. *Hematol Oncol* 2020; **38**: 12–21. doi: <https://doi.org/10.1002/hon.2676>
  65. Garbe C, Amaral T, Peris K, Hauschild A, Arenberger P, Bastholt L, et al. European consensus-based interdisciplinary guideline for melanoma. Part 1: Diagnostics - Update 2019. *Eur J Cancer* 2020; **126**: 141–58. doi: <https://doi.org/10.1016/j.ejca.2019.11.014>
  66. Li B, Li Q, Nie W, Liu S. Diagnostic value of whole-body diffusion-weighted magnetic resonance imaging for detection of primary and metastatic malignancies: a meta-analysis. *Eur J Radiol* 2014; **83**: 338–44. doi: <https://doi.org/10.1016/j.ejrad.2013.11.017>
  67. Ciliberto M, Maggi F, Treglia G, Padovano F, Calandriello L, Giordano A, et al. Comparison between whole-body MRI and fluorine-18-fluorodeoxyglucose PET or PET/CT in oncology: a systematic review. *Radiol Oncol* 2013; **47**: 206–18. doi: <https://doi.org/10.2478/raon-2013-0007>
  68. Petralia G, Padhani A, Summers P, Alessi S, Raimondi S, Testori A, et al. Whole-Body diffusion-weighted imaging: is it all we need for detecting metastases in melanoma patients? *Eur Radiol* 2013; **23**: 3466–76. doi: <https://doi.org/10.1007/s00330-013-2968-x>
  69. Pflugfelder A, Kochs C, Blum A, Capellaro M, Czeschik C, Dettenborn T, et al. Malignant Melanoma S3-Guideline “Diagnosis, Therapy and Follow-up of Melanoma”. *JDDG: Journal der Deutschen Dermatologischen Gesellschaft* 2013; **11**(s6): 1–116. doi: [https://doi.org/10.1111/ddg.12113\\_suppl](https://doi.org/10.1111/ddg.12113_suppl)
  70. Al Rawahi T, Lopes AD, Bristow RE, Bryant A, Elattar A, Chattopadhyay S, et al. Surgical cytoreduction for recurrent epithelial ovarian cancer. *Cochrane Database Syst Rev* 2013; **2**: CD008765.
  71. García Prado J, González Hernando C, Varillas Delgado D, Saiz Martínez R, Bhosale P, Blazquez Sanchez J, et al. Diffusion-Weighted magnetic resonance imaging in peritoneal carcinomatosis from suspected ovarian cancer: diagnostic performance in correlation with surgical findings. *Eur J Radiol* 2019; **121**: 108696. doi: <https://doi.org/10.1016/j.ejrad.2019.108696>
  72. Dresen RC, De Vuysere S, De Keyzer F, Van Cutsem E, Prenen H, Vanslebrouck R, et al. Whole-Body diffusion-weighted MRI for operability assessment in patients with colorectal cancer and peritoneal metastases. *Cancer Imaging* 2019; **19**: 1. doi: <https://doi.org/10.1186/s40644-018-0187-z>
  73. Rizzo S, De Piano F, Buscarino V, Pagan E, Bagnardi V, Zanagnolo V, et al. Pre-Operative evaluation of epithelial ovarian cancer patients: role of whole body diffusion weighted imaging Mr and CT scans in the selection of patients suitable for primary debulking surgery. A single-centre study. *Eur J Radiol* 2020; **123**: 108786. doi: <https://doi.org/10.1016/j.ejrad.2019.108786>
  74. Sepriano A, Rubio R, Ramiro S, Landewé R, van der Heijde D. Performance of the ASAS classification criteria for axial and peripheral spondyloarthritis: a systematic literature review and meta-analysis. *Ann Rheum Dis* 2017; **76**: 886–90. doi: <https://doi.org/10.1136/annrheumdis-2016-210747>
  75. Vilanova JC, García-Figueiras R, Luna A, Baleato-González S, Tomás X, Narváez JA. Update on whole-body MRI in musculoskeletal applications. *Semin Musculoskelet Radiol* 2019; **23**: 312–23. doi: <https://doi.org/10.1055/s-0039-1685540>
  76. Damasio MB, Magnaguagno F, Stagnaro G. Whole-Body MRI: non-oncological applications in paediatrics. *Radiol Med* 2016; **121**: 454–61. doi: <https://doi.org/10.1007/s11547-015-0619-9>
  77. Glinatsi D, Bird P, Gandjbakhch F, Mease PJ, Boyesen P, Peterfy CG, et al. Validation of the OMERACT psoriatic arthritis magnetic resonance imaging score (PsAMRIS) for the hand and foot in a randomized placebo-controlled trial. *J Rheumatol* 2015; **42**: 2473–9. doi: <https://doi.org/10.3899/jrheum.141010>
  78. Mathew AJ, Krabbe S, Eshed I, Gandjbakhch F, Bird P, Pedersen SJ, et al. The OMERACT MRI in Enthesitis initiative: definitions of key pathologies, suggested MRI sequences, and a novel heel Enthesitis scoring system. *J Rheumatol* 2019; **46**: 1232–8. doi: <https://doi.org/10.3899/jrheum.181093>
  79. Lai JKC, Robertson PL, Goh C, Szer J. Intraobserver and interobserver variability of the bone marrow burden (BMB) score for the assessment of disease severity in Gaucher disease. Possible impact of

- reporting experience. *Blood Cells Mol Dis* 2018; **68**: 121–5. doi: <https://doi.org/10.1016/j.bcmd.2016.11.004>
80. Krabbe S, Eshed I, Sørensen J I, Jensen B, Møller JM, Balding L, et al. Whole-Body magnetic resonance imaging inflammation in peripheral joints and Entheses in axial spondyloarthritis: distribution and changes during adalimumab treatment. *J Rheumatol*. 2019;.
  81. Axelsen MB, Eshed I, Østergaard M, Hetland ML, Møller JM, Jensen DV, et al. Monitoring total-body inflammation and damage in joints and entheses: the first follow-up study of whole-body magnetic resonance imaging in rheumatoid arthritis. *Scand J Rheumatol* 2017; **46**: 253–62. doi: <https://doi.org/10.1080/03009742.2016.1231338>
  82. Song I-H, Hermann K, Haibel H, Althoff CE, Althoff C, Listing J, et al. Effects of etanercept versus sulfasalazine in early axial spondyloarthritis on active inflammatory lesions as detected by whole-body MRI (ESTHER): a 48-week randomised controlled trial. *Ann Rheum Dis* 2011; **70**: 590–6. doi: <https://doi.org/10.1136/ard.2010.139667>
  83. Lecouvet FE, Vander Maren N, Collette L, Michoux N, Triqueneaux P, Stoeniou M, et al. Whole body MRI in spondyloarthritis (spa): preliminary results suggest that DWI outperforms stir for lesion detection. *Eur Radiol* 2018; **28**: 4163–73. doi: <https://doi.org/10.1007/s00330-018-5377-3>
  84. Neubauer H, Evangelista L, Morbach H, Girschick H, Prelog M, Köstler H, et al. Diffusion-Weighted MRI of bone marrow oedema, soft tissue oedema and synovitis in paediatric patients: feasibility and initial experience. *Pediatr Rheumatol Online J* 2012; **10**: 20. doi: <https://doi.org/10.1186/1546-0096-10-20>
  85. Barendregt AM, van Gulik EC, Lavini C, Nusman CM, van den Berg JM, Schonenberg-Meinema D, et al. Diffusion-Weighted imaging for assessment of synovial inflammation in juvenile idiopathic arthritis: a promising imaging biomarker as an alternative to gadolinium-based contrast agents. *Eur Radiol* 2017; **27**: 4889–99. doi: <https://doi.org/10.1007/s00330-017-4876-y>
  86. Bozgeyik Z, Ozgocmen S, Kocakoc E. Role of diffusion-weighted MRI in the detection of early active sacroiliitis. *AJR Am J Roentgenol* 2008; **191**: 980–6. doi: <https://doi.org/10.2214/AJR.07.3865>
  87. van Vucht N, Santiago R, Lottmann B, Pressney I, Harder D, Sheikh A, et al. The Dixon technique for MRI of the bone marrow. *Skeletal Radiol* 2019; **48**: 1861–74. doi: <https://doi.org/10.1007/s00256-019-03271-4>
  88. Roderick MR, Shah R, Rogers V, Finn A, Ramanan AV. Chronic recurrent multifocal osteomyelitis (CRMO) - advancing the diagnosis. *Pediatr Rheumatol Online J* 2016; **14**: 47. doi: <https://doi.org/10.1186/s12969-016-0109-1>
  89. Andronikou S, Mendes da Costa T, Hussien M, Ramanan AV. Radiological diagnosis of chronic recurrent multifocal osteomyelitis using whole-body MRI-based lesion distribution patterns. *Clin Radiol* 2019; **74**: 737.e3–737.e15. doi: <https://doi.org/10.1016/j.crad.2019.02.021>
  90. Maas M, van Kuijk C, Stoker J, Hollak CEM, Akkerman EM, Aerts JFMG, et al. Quantification of bone involvement in Gaucher disease: MR imaging bone marrow burden score as an alternative to Dixon quantitative chemical shift MR imaging-initial experience. *Radiology* 2003; **229**: 554–61. doi: <https://doi.org/10.1148/radiol.2292020296>
  91. Laudemann K, Moos L, Mengel E, Lollert A, Hoffmann C, Brixius-Huth M, et al. Evaluation of treatment response to enzyme replacement therapy with Velaglucerase alfa in patients with Gaucher disease using whole-body magnetic resonance imaging. *Blood Cells Mol Dis* 2016; **57**: 35–41. doi: <https://doi.org/10.1016/j.bcmd.2015.11.003>
  92. McLaughlin PD, Ryan J, Hodnett PA, O'Halloran D, Maher MM. Quantitative whole-body MRI in familial partial lipodystrophy type 2: changes in adipose tissue distribution coincide with biochemical improvement. *AJR Am J Roentgenol* 2012; **199**: W602–6. doi: <https://doi.org/10.2214/AJR.11.8110>
  93. Perez-Rossello JM, Connolly SA, Newton AW, Zou KH, Kleinman PK. Whole-Body MRI in suspected infant abuse. *AJR Am J Roentgenol* 2010; **195**: 744–50. doi: <https://doi.org/10.2214/AJR.09.3364>
  94. Boutin RD, White LM, Laor T, Spitz DJ, Lopez-Ben RR, Stevens KJ, et al. MRI findings of serous atrophy of bone marrow and associated complications. *Eur Radiol* 2015; **25**: 2771–8. doi: <https://doi.org/10.1007/s00330-015-3692-5>
  95. Ruder TD, Thali MJ, Hatch GM. Essentials of forensic post-mortem MR imaging in adults. *Br J Radiol* 2014; **87**: 20130567. doi: <https://doi.org/10.1259/bjr.20130567>
  96. Donners R, Blackledge M, Tunariu N, Messiou C, Merkle EM, Koh D-M. Quantitative whole-body diffusion-weighted MR imaging. *Magn Reson Imaging Clin N Am* 2018; **26**: 479–94. doi: <https://doi.org/10.1016/j.mric.2018.06.002>
  97. Perez-Lopez R, Nava Rodrigues D, Figueiredo I, Mateo J, Collins DJ, Koh D-M, et al. Multiparametric magnetic resonance imaging of prostate cancer bone disease: correlation with bone biopsy histological and molecular features. *Invest Radiol* 2018; **53**: 96–102. doi: <https://doi.org/10.1097/RLI.0000000000000415>
  98. Galbán CJ, Hoff BA, Chenevert TL, Ross BD. Diffusion MRI in early cancer therapeutic response assessment. *NMR Biomed* 2017; **30**: e345815 01 2016. doi: <https://doi.org/10.1002/nbm.3458>
  99. Zormpas-Petridis K, Tunariu N, Messiou C, Koh D-M, Jamin Y, Blackledge M. Accelerating Whole-Body Diffusion-Weighted MRI with Artificial Intelligence. In: *2019 Scientific Assembly and Annual Meeting*. IL. Chicago: Radiological Society of North America; 2019. pp. 2019.
  100. Blackledge MD, Koh DM, Collins DJ, Scurr E, Hughes J, Leach MO, et al. Assessing response heterogeneity following radium 223 administration using whole body diffusion weighted MRI. *ISMRM* 2017; **22-27**(April).